JACS
JOURNAL OF THE AMERICAN CHEMICAL SOCIETY
Communication
pubs.acs.org/JACS

Selective Gold Recovery and Catalysis in a Highly Flexible Methionine-Decorated Metal–Organic Framework

Marta Mon,[†] Jesús Ferrando-Soria,[†] Thais Grancha,[†] Francisco R. Fortea-Pérez,[†] Jorge Gascon,[⊥] Antonio Leyva-Pérez,*[,‡] Donatella Armentano,*[,§] and Emilio Pardo*[,†]

[†]Departament de Química Inorgànica, Instituto de Ciencia Molecular (ICMOL), Universitat de València, 46980 Paterna, València, Spain

[⊥]Catalysis Engineering Department, Delft University of Technology, Julianalaan 136, 2628 BL Delft, The Netherlands

[‡]Instituto de Tecnología Química (UPV-CSIC), Universitat Politècnica de València-Consejo Superior de Investigaciones Científicas, Avda. de los Naranjos s/n, 46022 Valencia, Spain

[§]Dipartimento di Chimica e Tecnologie Chimiche (CTC), Università della Calabria, Rende 87036, Cosenza, Italy

Supporting Information

ABSTRACT: A novel chiral 3D bioMOF exhibiting functional channels with thio-alkyl chains derived from the natural amino acid L-methionine (**1**) has been rationally prepared. The well-known strong affinity of gold for sulfur derivatives, together with the extremely high flexibility of the thioether "arms" decorating the channels, account for a selective capture of gold(III) and gold(I) salts in the presence of other metal cations typically found in electronic wastes. The X-ray single-crystal structures of the different gold adsorbates $\mathbf{Au^{III}@1}$ and $\mathbf{Au^{I}@1}$ suggest that the selective metal capture occurs in a metal ion recognition process somehow mimicking what happens in biological systems and protein receptors. Both $\mathbf{Au^{III}@1}$ and $\mathbf{Au^{I}@1}$ display high activity as heterogeneous catalyst for the hydroalkoxylation of alkynes, further expanding the application of these novel hybrid materials.

The consumerism that modern societies have developed toward electronics devices has transformed the electronic waste into urban mines for noble metals. In particular, the recovery of gold from electronic scraps is extremely important from an economic and environmental perspective.[1] The high concentration of gold in electronic wastes has driven the quest of environmentally friendly methods for the recovery of gold from aqueous solutions. Although very few alternative methods to the highly contaminating cyanide leeching[2] have been proposed,[3,4] further advances focusing on increasing gold-selectivity and chemicals saving are mandatory.

Metal–organic frameworks (MOFs)[5−9] are porous materials showing a wide variety of thrilling chemical and physical properties and, consequently, find applications in very diverse fields.[10−15] Indeed, both MOF's porosity and their fascinating host–guest chemistry[14] lie at the origin of most of these properties. In the same way that other porous materials,[16,17] MOFs have proven their efficiency as vessels to capture and host small molecules[18] and, eventually, to separate mixtures of molecules according to their steric and stereochemical features as well as reactivity properties (functional substituent groups).[19−22]

Despite the fact that a few examples of selective metal capture by MOFs have been reported,[23] to the best of our knowledge, the important recovery of Au has not been studied. Aiming at expanding the scope of application of MOFs and taking advantage of the well-known strong affinity of gold for sulfur derivatives,[24,25] we have focused our efforts on the rational design of bioMOFs showing functional channels decorated with thio-alkyl chains derived from the natural amino acid[26] L-methionine (Scheme S1). Thus, we have synthesized a robust and water-stable 3D bioMOF of formula $\{Ca^{II}Cu^{II}_6[(S,S)\text{-methox}]_3(OH)_2(H_2O)\}\cdot 16H_2O$ (**1**). The presence of thioether groups within the accessible void space of this porous material encouraged us to evaluate its selectivity for the recovery of gold. Indeed, **1** exhibited a great affinity for Au^{3+} and Au^{+} salts (such as $AuCl_3$ and AuCl) in water, even in the presence of a wide variety of other metal cations regularly present in electronic wastes ("e-wastes") like Pd^{2+}, Ni^{2+}, Cu^{2+}, Zn^{2+} and Al^{3+}, yielding the novel compounds $(AuCl_3)_3@\{Ca^{II}Cu^{II}_6[(S,S)\text{-methox}]_3(OH)_2(H_2O)\}\cdot 9H_2O$ ($\mathbf{Au^{III}@1}$) and $(AuCl)_2@\{Ca^{II}Cu^{II}_6[(S,S)\text{-methox}]_3(OH)_2(H_2O)\}\cdot 3H_2O\cdot 3CH_3OH$ ($\mathbf{Au^{I}@1}$) (see Supporting Information (SI)).

Compound **1** was synthesized as green hexagonal prisms with a slow diffusion technique (see experimental section in the SI). Thereafter, in order to find out the maximum gold uptake capacity, we suspended 5 mg of **1** in 5 mL of a 0.02 M $AuCl_3$ H_2O/CH_3OH (1:1) solution to obtain $\mathbf{Au^{III}@1}$. ICP-AES and SEM analyses indicated a maximum loading of 3 mmol of Au(III) per mmol of MOF after 1 h, which remained invariable after further time suspension. This indicates a total recovery of 598 mg of $AuCl_3$ per g of MOF in $\mathbf{Au^{III}@1}$. The same procedure was repeated by soaking 5 mg of **1** in 5 mL of a 0.02 M AuCl aqueous solution. A maximum uptake of two mmol of AuCl per mmol of MOF was achieved after 3 h. The calculated total recovery of 300 mg of AuCl per g of MOF in $\mathbf{Au^{I}@1}$ is almost half-fold to that of $\mathbf{Au^{III}@1}$.

The crystal structures of **1**, $\mathbf{Au^{III}@1}$ and $\mathbf{Au^{I}@1}$ could be determined by single-crystal X-ray diffraction (XRD) (see SI for structural details). They crystallize in the chiral $P6_3$ space group

Received: May 11, 2016
Published: June 13, 2016

DOI: 10.1021/jacs.6b04635
J. Am. Chem. Soc. 2016, 138, 7864−7867

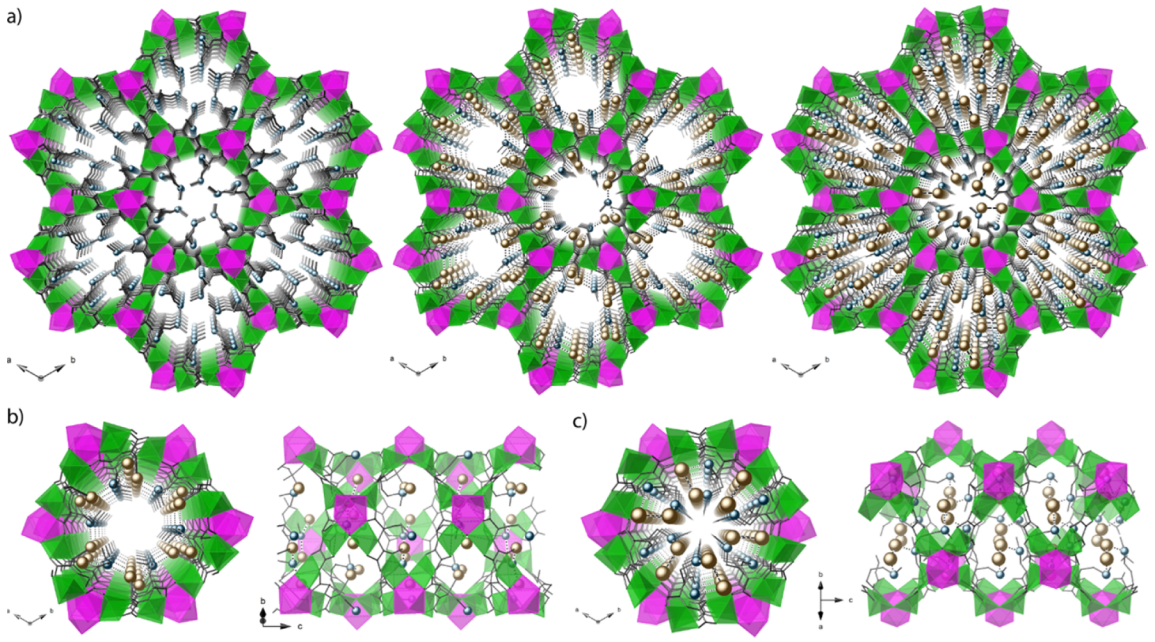

Figure 1. (a) Perspective views along the *c* axis of the porous structure of **1** (left), **Au^{III}@1** (center), and **Au^{I}@1** (right) determined by single-crystal XRD. Top (left) and lateral (right) views of one channel of **Au^{III}@1** (b) and **Au^{I}@1** (c). Copper and calcium atoms are represented by green and purple octahedra, respectively, whereas gold and sulfur atoms have been depicted as yellow and blue spheres. Free solvent molecules and Cl^- counterions are omitted for clarity.

and consist of honeycomb-like three-dimensional (3D) calcium(II)−copper(II) networks (Figure 1).

The network of **1** shows hexagonal channels of ∼0.3 nm as virtual diameter featuring highly flexible ethylenethiomethyl arms, belonging to the amino acid residues of methionine-disubstituted oxamidato ligand, which remain confined, together with lattice water molecules, in the pores of the MOF (Figure 1a, left and Figures S1 and S2a). The structures of **Au^{III}@1** and **Au^{I}@1**, determined by single-crystal XRD, confirm the preservation of the network of **1** even after gold capture. Delightfully, both of them host in the pores Au^{I} (**Au^{I}@1**) and Au^{III} ions (**Au^{III}@1**) clenched by methionine derivative arms (Figure 1b,c).

The gold(I) atoms in **Au^{I}@1** are two-coordinated, clutched by the sulfur atom from the two thioether arms and additional bridging chlorine atoms in a quite linear geometry of the S−Au−Cl type at the distended arm, whereas highly distorted, likely for steric constrains imposed by the network, at the more bent ones (Figures S2b and S3a). In contrast, the gold(III) atoms in **Au^{III}@1** are connected to the sulfur atom from only one of the two thioether arms and further bounded to three chloride atoms (two of them were not found from ΔF map, see crystallographic section in SI) in an expected distorted square planar coordination geometry (Figures S2b and S3b). The average Au−S bond distances of 2.75(7) (**Au^{I}@1**)/2.80(3) Å (**Au^{III}@1**) are somewhat longer than those reported so far for Au^{III}, whereas the Au−Cl ones of 2.50(7) (**Au^{I}@1**)/2.19(2) Å (**Au^{III}@1**) fall in the typical range of related gold(I) and gold(III) compounds found in the literature.[27−29] Aurophilic interactions[30] are present in **Au^{I}@1**, the shortest Au···Au separations being 3.04(2) Å (Figures S4 and S5).

As a striking structural uniqueness of this series of bioMOFs, they showed a permanent highly stable 3D net, featuring highly flexible arms able to arrange in different conformations of the thioether chains depending on the different chemical environments of the metal guests. The amino acid methionine side-chains remain available in the accessible voids of the bioMOF getting ready for metal ions recognition processes (Figure S6). The thioether "arms" are shown to adopt a stable conformation and target metals with high affinity, which is reminiscent of that seen in biological systems and protein receptors. They feature a sulfur available linkage which finally coordinates the desired metal assuming the favorite conformation. In fact, even if the honeycomb-like hexagonal 3D $Ca^{II}Cu^{II}_6$ network of **Au^{III}@1** and **Au^{I}@1** is basically the same of **1**, the thioether-containing arms exhibit a different conformation when holding the Au^{3+} and Au^{+} ions compared to the original material (see SI for structural details and Figures S1, S2, S6, and S7). Besides, only one of the two arms binds directly Au^{3+} in **Au^{III}@1**, the other being weakly bounded to Cl [S···Cl = 2.50(1) Å] and thus contributing through chlorine bridges to capture Au^{3+} in its second sphere of coordination (Figure S8) and forcing the folding of the flexible ethylenethiomethyl chains in a highly bent conformation of methyl groups and their overall arrangement pointing along *c* axis and not inward the pores (Figures S2c, S3b, and S6c). Hence, the virtual diameter of the channels is slightly increased after metal loading in **Au^{III}@1** (likely at the origin of disordered chloride atoms) in comparison to **1** and **Au^{I}@1** [∼0.3 (**1**), 0.2 (**Au^{I}@1**), and 0.6 nm (**Au^{III}@1**)], even if the estimated empty volumes without the crystallization solvent molecules decrease as expected in both **Au^{III}@1** and **Au^{I}@1** adsorbates [1101.4 (**1**), 776.2 (**Au^{I}@1**) and 609.8 $Å^3$ (**Au^{III}@1**) (Figures S1 and S7).

The experimental powder XRD (PXRD) patterns of **1**, **Au^{III}@1**, and **Au^{I}@1** are shown in Figure S9b,d,f, respectively. They are in agreement with the theoretical ones (Figure S9a,c,e), confirming the purity and homogeneity of the bulk samples. Solvent contents of both materials were estimated by thermogravimetric analysis under dry N_2 atmosphere (see Figure S10). Finally, Figure S11 shows the N_2 adsorption isotherms of **1**, **Au^{III}@1**, and **Au^{I}@1** at 77 K. They are consistent with the decrease in accessible void space in **Au^{III}@1** and **Au^{I}@1** estimated from the analysis of the crystal structure.

DOI: 10.1021/jacs.6b04635
J. Am. Chem. Soc. 2016, 138, 7864−7867

Aiming at evaluating the selectivity of **1** in gold(III) capture as well as the kinetics of the process, we then monitored the insertion of $AuCl_3$ within the pores of **1**, through ICP-AES and SEM, by soaking both powder and single-crystals of **1** in an equimolar aqueous solution of $AuCl_3$, $[Pd(NH_3)_4]Cl_2$, $NiCl_2$, $CuCl_2$, $ZnCl_2$, and $AlCl_3$ (see Figure 2 and SI). The kinetics of

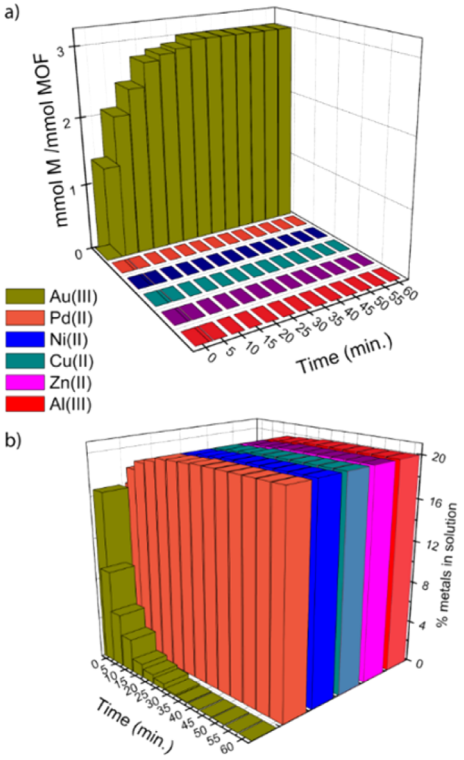

Figure 2. Kinetic profile of the selective gold(III) recovery by **1** represented as the mmol M/mmol MOF vs time (a) and the remaining % of metal cations in the aqueous solution vs time (b).

insertion was followed through both the increase of the mmol M/mmol MOF ratio (M = Au^{III}, Pd^{II}, Ni^{II}, Cu^{II}, Zn^{II} and Al^{III}) within the MOF (Figure 2a and Table S2) and the metal ratio (%) within the aqueous solution (Figure 2b and Table S3) at specific time intervals (0−60 min) of immersion of **1** in the aqueous solutions. A very selective and fast insertion of $AuCl_3$ within the MOF was observed, whereas all the other metal salts remained in solution. After only 5 min, a 67% of the maximum loading is achieved (Figure 2a). The maximum loading is finally reached after 30 min of soaking (3 mmol $AuCl_3$ per mmol MOF). In good agreement with solid data, ICP-AES and SEM indicate a continuous decrease of $[AuCl_3]$ within the aqueous solution, almost to a halt after 30 min of soaking (Figure 2b). Overall, the recovery efficiency of this material is close to 100%.

The same methodology was followed to test the selectivity of **1** in gold(I) capture by using the same equimolar aqueous solution but replacing $AuCl_3$ by partially dissolved AuCl (Figure S12). As expected, **1** also showed a great affinity and selectivity for AuCl in the presence of other metal salts. A maximum loading of 2 mmol of AuCl per mmol of MOF was achieved after 3 h, with a concomitant redissolution of the excess of suspended AuCl (Figure S12a and Table S4). The kinetic profile for the insertion of AuCl within the MOF indicates a somewhat slower process when compared to what happens to $AuCl_3$ (Figure S12b and Table S5). More likely, this fact can be attributed to the poor solubility of AuCl. Finally, both gold(III) and gold(I) salts were easily extracted from **Au^{III}@1** and **Au^{I}@1** by soaking them in a sulfur-containing solvent (i.e., dimethylsulfide), so that the resulting starting material (**1**) was completely reusable as confirmed by ICP and elemental analyses as well as the PXRD pattern of the material (**1′**) after the extraction process (Figure S13).

The extremely high loading of gold cations (15−20 wt %) supported on **Au^{III}@1** and **Au^{I}@1** is unprecedented in solids, as far as we know.[31] Thus, these new materials could be high-throughput heterogeneous catalysts in AuCl- and $AuCl_3$-catalyzed reactions, such as the hydroalkoxylation of alkynes[31,32] or the formation of related spiroketals, which have shown the highest turnover numbers in the field of homogeneous gold catalysis.[33−35]

Figure 3a shows that **Au^{III}@1** and **Au^{I}@1** catalyze the cyclization/ketalization of 4-pentyn-1-ol under standard con-

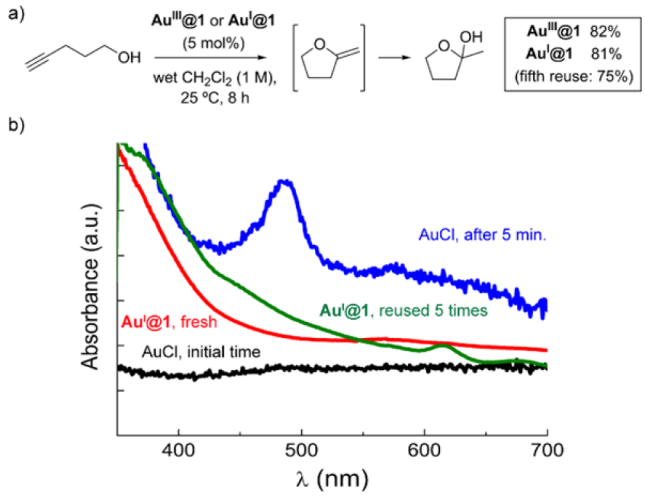

Figure 3. (a) Hydroalkoxylation of 4-pentyn-1-ol in wet CH_2Cl_2 catalyzed by **Au^{III}@1** and **Au^{I}@1**. (b) Visible region of the UV−vis and RD measurements.

ditions (wet CH_2Cl_2 as a solvent, 1 M, room temperature) in good yield and selectivity, even after five reuses and without any leaching of gold detected by a filtration test (Figure S14). Kinetic experiments show that **Au^{III}@1** gives higher initial rates than **Au^{I}@1**, in accordance with the higher Lewis acidity and wider porous size of the former. A first-order reaction with respect to the gold catalyst with a smooth langmuirian curve only saturated at yields >70% is also observed (Figure S15a).

Comparatively, the homogeneous reaction with AuCl shows an abrupt stopping of the conversion at around 60% yield, regardless the amount of gold salt employed (Figure S15b). This homogeneous reaction was followed by in situ UV−vis spectroscopy measurements (Figure 3b). A new band in the visible region at ∼500 nm denotes the generation of spherical plasmonic nanoparticles in just 5 min, which suggests that the reaction stops as consequence of the very fast agglomeration of AuCl in the form of catalytically inactive nanoparticles. In contrast, diffuse-reflectance spectroscopy measurements of the reused **Au^{I}@1** material show the absence of this plasmonic band (see also Figure S16), demonstrating the advantage of site isolation upon anchoring the Au salts to the thioether groups within the MOF structure. The small peak at ∼620 nm can be related to the reduction of a negligible amount of Au^{I} cations to plasmonic gold nanorods.[36]

DOI: 10.1021/jacs.6b04635
J. Am. Chem. Soc. 2016, 138, 7864−7867

In summary, we report an environmentally friendly, cheap, and easy-to-prepare in large-scale MOF whose channels are decorated with thioether groups. This material exhibits a high selectivity for $AuCl_3$ and AuCl, even in the presence of other metal cations regularly present in "e-wastes" such as Pd^{2+}, Ni^{2+}, Cu^{2+}, Zn^{2+}, and Al^{3+}, in a fully reversible process. The nature and kinetics of these postsynthetic selective processes have been evaluated. The structural stability of the 3D network of **1**, maintaining the crystallinity over the inclusion processes, allowed the resolution of the crystal structures of the corresponding final products $\mathbf{Au^{III}}$**@1** and $\mathbf{Au^{I}}$**@1**, permitting structural insights into the nature of the Au−S interaction and the flexibility and adaptability of the material. In addition, both compounds show excellent performance as reusable heterogeneous catalysts for the intramolecular hydroalkoxylation of alkynes. These results demonstrate the great versatility of MOFs in separation and further expand the scope of application of these unique class of porous materials.

■ ASSOCIATED CONTENT

Supporting Information

The Supporting Information is available free of charge on the ACS Publications website at DOI: 10.1021/jacs.6b04635.

Preparation and characterization of **1**, $\mathbf{Au^{III}}$**@1** and $\mathbf{Au^{I}}$**@1**. Experimental details of metal selectivity experiences. Additional Figures S1−S16. CCDC reference numbers 1478221−1478223 for **1**, $\mathbf{Au^{III}}$**@1** and $\mathbf{Au^{I}}$**@1** (PDF)
Crystallographic data (CIF)
Crystallographic data (CIF)
Crystallographic data (CIF)

■ AUTHOR INFORMATION

Corresponding Authors

*emilio.pardo@uv.es
*donatella.armentano@unical.it
*anleyva@itq.upv.es

Notes

The authors declare no competing financial interest.

■ ACKNOWLEDGMENTS

This work was supported by the MINECO (Spain) (Projects CTQ2013-46362-P, CTQ2013-44844-P, and Excellence Unit "Maria de Maeztu" MDM-2015-0538), the Generalitat Valenciana (Spain) (Project PROMETEOII/2014/070), and the Ministero dell'Istruzione, dell'Università e della Ricerca (Italy). M.M. and T.G. thank the MINECO and the Universitat de València for predoctoral contracts. Thanks are also extended to the Ramón y Cajal Program and the "Convocatoria 2015 de Ayudas Fundación BBVA a Investigadores y Creadores Culturales" (E. P., A. L.-P., and J. F.-S.). J.G. acknowledges the financial support of the European Research Council: FP/2007-2013 and ERC grant agreement no. 335746, CrystEng-MOF-MMM.

■ REFERENCES

(1) Hagelüken, C.; Corti, C. W. *Gold Bull.* **2010**, *43*, 209.
(2) Syed, S. *Hydrometallurgy* **2012**, *115−116*, 30.
(3) Liu, Z.; Frasconi, M.; Lei, J.; Brown, Z. J.; Zhu, Z.; Cao, D.; Iehl, J.; Liu, G.; Fahrenbach, A. C.; Botros, Y. Y.; Farha, O. K.; Hupp, J. T.; Mirkin, C. A.; Fraser Stoddart, J. *Nat. Commun.* **2013**, *4*, 1855.
(4) He, Y.-R.; Cheng, Y.-Y.; Wang, W.-K.; Yu, H.-Q. *Chem. Eng. J.* **2015**, *270*, 476.
(5) Férey, G. *Chem. Soc. Rev.* **2008**, *37*, 191.
(6) Long, J. R.; Yaghi, O. M. *Chem. Soc. Rev.* **2009**, *38*, 1213.
(7) Furukawa, H.; Cordova, K. E.; O'Keeffe, M.; Yaghi, O. M. *Science* **2013**, *341*, 1230444.
(8) Eddaoudi, M.; Sava, D. F.; Eubank, J. F.; Adil, K.; Guillerm, V. *Chem. Soc. Rev.* **2015**, *44*, 228.
(9) Cui, Y.; Li, B.; He, H.; Zhou, W.; Chen, B.; Qian, G. *Acc. Chem. Res.* **2016**, *49*, 483.
(10) Li, J.; Sculley, J.; Zhou, H. *Chem. Rev.* **2012**, *112*, 869.
(11) Horike, S.; Umeyama, D.; Kitagawa, S. *Acc. Chem. Res.* **2013**, *46*, 2376.
(12) McKinlay, A. C.; Morris, R. E.; Horcajada, P.; Férey, G.; Gref, R.; Couvreur, P.; Serre, C. *Angew. Chem., Int. Ed.* **2010**, *49*, 6260.
(13) Grancha, T.; Ferrando-Soria, J.; Castellano, M.; Julve, M.; Pasán, J.; Armentano, D.; Pardo, E. *Chem. Commun.* **2014**, *50*, 7569.
(14) Inokuma, Y.; Arai, T.; Fujita, M. *Nat. Chem.* **2010**, *2*, 780.
(15) Gascon, J.; Corma, A.; Kapteijn, F.; Llabrés i Xamena, F. X. *ACS Catal.* **2014**, *4*, 361.
(16) Cote, A. P.; Benin, A. I.; Ockwig, N. W.; O'Keeffe, M.; Matzger, A. J.; Yaghi, O. M. *Science* **2005**, *310*, 1166.
(17) Slater, A. G.; Cooper, A. I. *Science* **2015**, *348*, aaa8075.
(18) Ferrando-Soria, J.; Serra-Crespo, P.; de Lange, M.; Gascon, J.; Kapteijn, F.; Julve, M.; Cano, J.; Lloret, F.; Pasán, J.; Ruiz-Pérez, C.; Journaux, Y.; Pardo, E. *J. Am. Chem. Soc.* **2012**, *134*, 15301.
(19) Yang, S.; Ramirez-Cuesta, A. J.; Newby, R.; Garcia-Sakai, V.; Manuel, P.; Callear, S. K.; Campbell, S. I.; Tang, C. C.; Schröder, M. *Nat. Chem.* **2014**, *7*, 121.
(20) Alezi, D.; Peedikakkal, A. M. P.; Weseliński, Ł. J.; Guillerm, V.; Belmabkhout, Y.; Cairns, A. J.; Chen, Z.; Wojtas, Ł.; Eddaoudi, M. *J. Am. Chem. Soc.* **2015**, *137*, 5421.
(21) Foo, M. L.; Matsuda, R.; Hijikata, Y.; Krishna, R.; Sato, H.; Horike, S.; Hori, A.; Duan, J.; Sato, Y.; Kubota, Y.; Takata, M.; Kitagawa, S. *J. Am. Chem. Soc.* **2016**, *138*, 3022.
(22) Seoane, B.; Castellanos, S.; Dikhtiarenko, A.; Kapteijn, F.; Gascon, J. *Coord. Chem. Rev.* **2016**, *307*, 147.
(23) Yuan, S.; Chen, Y.-P.; Qin, J.; Lu, W.; Wang, X.; Zhang, Q.; Bosch, M.; Liu, T.-F.; Lian, X.; Zhou, H.-C. *Angew. Chem., Int. Ed.* **2015**, *54*, 14696.
(24) Häkkinen, H. *Nat. Chem.* **2012**, *4*, 443.
(25) Xue, Y.; Li, X.; Li, H.; Zhang, W. *Nat. Commun.* **2014**, *5*, 4348.
(26) Grancha, T.; Ferrando-Soria, J.; Cano, J.; Lloret, F.; Julve, M.; De Munno, G.; Armentano, D.; Pardo, E. *Chem. Commun.* **2013**, *49*, 5942.
(27) Blake, A. J.; Gould, R. O.; Greig, J. A.; Holder, A. J.; Hyde, T. I.; Schröder, M. *J. Chem. Soc., Chem. Commun.* **1989**, 876.
(28) Grirrane, A.; Álvarez, E.; García, H.; Corma, A. *Angew. Chem., Int. Ed.* **2014**, *53*, 7253.
(29) Yang, S.; Chai, J.; Song, Y.; Kang, X.; Sheng, H.; Chong, H.; Zhu, M. *J. Am. Chem. Soc.* **2015**, *137*, 10033.
(30) Schmidbaur, H. *Chem. Soc. Rev.* **1995**, *24*, 391.
(31) Corma, A.; Leyva-Pérez, A.; Sabater, M. J. *Chem. Rev.* **2011**, *111*, 1657.
(32) Trost, B. M.; Dong, G. *Nature* **2008**, *456*, 485.
(33) Hashmi, A. S. K. *Science* **2012**, *338*, 1434.
(34) Blanco Jaimes, M. C.; Böhling, C. R. N.; Serrano-Becerra, J. M.; Hashmi, A. S. K. *Angew. Chem., Int. Ed.* **2013**, *52*, 7963.
(35) Blanco Jaimes, M. C.; Rominger, F.; Pereira, M. M.; Carrilho, R. M. B.; Carabineiro, S. A. C.; Hashmi, A. S. K. *Chem. Commun.* **2014**, *50*, 4937.
(36) Pérez-Juste, J.; Pastoriza-Santos, I.; Liz-Marzán, L.; Mulvaney, P. *Coord. Chem. Rev.* **2005**, *249*, 1870.

DOI: 10.1021/jacs.6b04635
J. Am. Chem. Soc. 2016, 138, 7864−7867